

Reactions of Molybdenocene and Tungstenocene Derivatives with Cobalt Carbonyls and the Related Compounds

Takashi Nakamura, Makoto Minato, Takashi Ito,* Masako Tanaka,† and Kohtaro Osakada†

Department of Materials Chemistry, Faculty of Engineering, Yokohama National University,
79-5 Tokiwadai, Yokohama 240

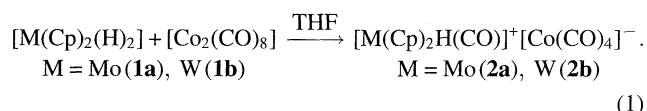
†Research Laboratory of Resources Utilization, Tokyo Institute of Technology, 4259 Nagatsuta, Midori-ku, Yokohama 226

(Received June 18, 1996)

Reactions of molybdenocene and tungstenocene derivatives $[\text{M}(\text{Cp})_2(\text{H})_2]$, $[\text{M}(\text{Cp})_2\text{H}(\text{OTs})]$, or $\{[\text{M}(\text{Cp})_2\text{H}(\mu\text{-Li})]_4\}$ ($\text{M} = \text{Mo}, \text{W}$) with $[\text{Co}_2(\text{CO})_8]$ or $[\text{Co}(\text{CO})_4]^-$ gave $[\text{M}(\text{Cp})_2\text{H}(\text{CO})]^+[\text{Co}(\text{CO})_4]^-$ and $[\text{M}(\text{Cp})_2(\mu\text{-H})(\mu\text{-CO})\text{Co}(\text{CO})_3]$ depending on the reaction conditions employed. These ionic heterobimetallic complexes were characterized by IR and NMR, as well as by X-ray diffraction analyses. A possible mechanism for the formation of the complexes is proposed.

Early/late heterobimetallic transition metal complexes have been known for many years and have represented an important group of compounds, which are interesting in view of their structure and bonding. Such complexes have been intensively investigated as a potentially new class of catalytic agents which may serve to activate small molecules such as H_2 , CO , C_2H_2 , or C_2H_4 . Bimetallic complexes which contain cobalt carbonyl moiety are currently of great interest because they are closely related to the hydroformylation reaction.¹⁾

Moise and co-workers reported that the bis(η^5 -cyclopentadienyl)dihydrido-molybdenum and -tungsten $[\text{M}(\text{Cp})_2(\text{H})_2]$ ($\text{Cp} = \eta^5\text{-C}_5\text{H}_5$, $\text{M} = \text{Mo}$ (**1a**), W (**1b**)), which display extensive reactivity with organic substrates and are useful starting materials for the preparation of molybdenocene and tungstenocene complexes,²⁾ reacted with $[\text{Co}_2(\text{CO})_8]$ to give novel ionic complexes $[\text{M}(\text{Cp})_2\text{H}(\text{CO})]^+[\text{Co}(\text{CO})_4]^-$ ($\text{M} = \text{Mo}$ (**2a**), W (**2b**))³⁾ (Eq. 1).



More recently, Nicholas and co-workers reported that the complex ($\text{M} = \text{Mo}$) was prepared by reaction between carbon dioxide complex $[\text{Mo}(\text{Cp})_2(\eta^2\text{-CO}_2)]$ and $[\text{CoH}(\text{CO})_4]$.^{4,5)} However, a detailed understanding of the structure of these complexes is still lacking and the reaction mechanism is also obscure. Our interest in the syntheses of molybdenocene and tungstenocene complexes^{6,7)} led us to examine the synthesis and structure of the complexes **2**. We describe here another synthetic route and the detailed characterization, including a single crystal X-ray study, of these complexes. The mechanism of the formation is also discussed.

Results and Discussion

Since there was no detailed description as to the syntheses

of the ionic complexes **2** in Moise and co-workers' communication, we investigated the reaction system in depth in order to find optimum conditions. The best results were obtained in the following manner. A solution of 2 molar amounts of $[\text{M}(\text{Cp})_2(\text{H})_2]$ and 1 molar amount of $[\text{Co}_2(\text{CO})_8]$ in THF was stirred at ambient temperature under argon. During the stirring, the solution color changed from red to dark-red. After being stirred for 12 h, the product was purified via recrystallization from THF– Et_2O . This procedure gave **2a** and **2b** in 50 and 43% yields, respectively. The spectroscopic properties of the complexes **2a** and **2b** were in accord with those reported by Moise and co-workers.³⁾ The IR spectra of **2a** and **2b** show sharp CO bands at 2030 and 2015 cm^{-1} , respectively, assignable to the molybdenum or tungsten bound CO's. The former is at higher frequency than that of the related mononuclear ionic complex $[\text{Mo}(\text{Cp})_2\text{H}(\text{CO})]^+(\text{OTs})^-$ ($\text{OTs} = p\text{-CH}_3\text{C}_6\text{H}_4\text{SO}_3$) (**3**) by about 30 cm^{-1} .⁸⁾ The CO stretching band of $[\text{Co}(\text{CO})_4]^-$ anion fragment appeared at 1880 cm^{-1} . The ^1H NMR spectrum of **2a** in THF- d_8 shows two singlet peaks at $\delta = -8.3$ assignable to Mo–H resonance and at $\delta = 5.7$ assignable to Cp ligands. These values are in good agreement with those found in **3**. The hydridic W–H protons of **2b** appeared as a singlet at $\delta = -10.1$ with ^{183}W satellites ($^1J_{\text{WP}} = 69$ Hz), which is at higher field than the molybdenum complex **2a**, reflecting a difference in the nature of metals; a similar feature was observed in the case of hydridophosphine complexes $[\text{M}(\text{Cp})_2\text{H}(\text{PR}_3)]^+(\text{OTs})^-$.⁶⁾

The molecular structures of the complexes **2a** and **2b** were confirmed by single crystal X-ray analyses. Crystals contain discrete $[\text{M}(\text{Cp})_2\text{H}(\text{CO})]^+$ and $[\text{Co}(\text{CO})_4]^-$ ions. Figure 1 shows the ORTEP drawing of the molybdenum complex **2a** with the numbering scheme for the atoms. This drawing will also serve to represent the tungsten complex **2b**, since the only differences are slight changes in some internuclear distances and angles, and the atom numbering schemes are parallel. Selected interatomic bond distances and angles are

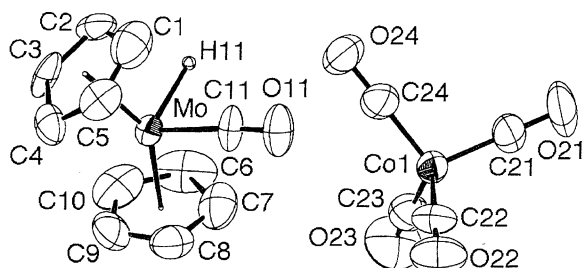


Fig. 1. ORTEP drawing of complex **2a** with atom-numbering scheme.

presented in Table 1.

These complexes have a monoclinic system. As shown in Fig. 1, the cationic part of the molecule consists of two Cp rings, which are coordinated to molybdenum or tungsten in a mutually eclipsed conformation, a carbonyl and a hydride. The distance from Mo to carbonyl carbon is 1.98(2) Å and is very similar to that found in the known complex $[\text{Mo}(\text{Cp})_2\text{H}(\text{CO})]^+[\text{MoCp}(\text{CO})_3]^-$ (**4**) (1.991 Å).⁹ The average value of the M–CP (CP is the centroid of the cyclopentadienyl ligand) distance is 1.937 Å in **2a** and 1.948 Å in **2b**. The CP–Mo–CP angle of 145.7° for **2a** is considerably larger than that found in typical $[\text{M}(\text{Cp})_2\text{X}_2]$ complexes⁷ and it is very close to that found in **4** (144.5°). Consequently, the structure of the cation $[\text{Mo}(\text{Cp})_2\text{H}(\text{CO})]^+$ seems to be not influenced by the anionic part of the complex. The CP–W–CP angle of 142.5° in **2b** is significantly smaller than the corresponding value of **2a**. These results suggest that steric repulsion among Cp rings of **2b** is smaller than that of **2a**. The average C–C bond distances of the Cp ring in **2a** (1.38 Å) and in **2b** (1.39 Å) are in accord with the accepted value. The

internal C–C–C ring angles in **2a** range from 103 to 112° and in **2b** from 103 to 113°. These angles are compared favorably with the expected internal angle, 108°, for a planar pentagon; hence, the cyclopentadienyl rings are bound to central metals in an η^5 fashion. The molybdenum–cobalt or tungsten–cobalt interaction is considered to be non-bonding since the observed separations (5.73 Å (**2a**) and 5.68 Å (**2b**)) are substantially longer than both M–Co distances of 2.46 Å (M=Mo, W), estimated from the sum of covalent radii.¹⁰

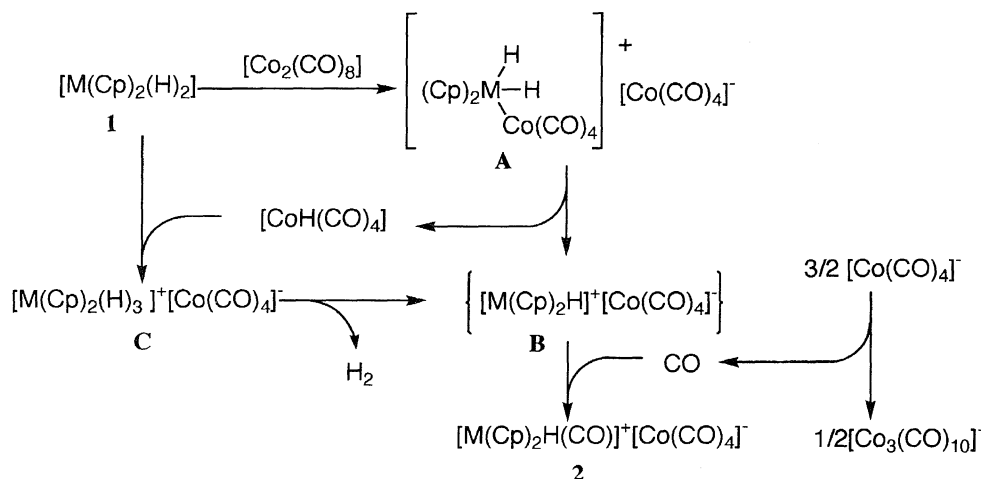
The structure of $[\text{Co}(\text{CO})_4]^-$ anion can be contrasted with that of the known tetracarbonylcobaltate complex $\text{Ti}[\text{Co}(\text{CO})_4]_4$,¹¹ and reveals tetrahedral coordination with four CO ligands. The Co–C distances in **2a** range from 1.69 to 1.73 Å and in **2b** from 1.73 to 1.74 Å. These distances are equal within experimental error and are shorter than that of $\text{Ti}[\text{Co}(\text{CO})_4]_4$ by ca. 0.1 Å. The average C–O bond distances in **2a** (1.17 Å) and in **2b** (1.12 Å) are significantly shorter than those found in the thallium(I) complex (1.23 Å).¹¹ The Co–C–O bond angles average 178° in both **2a** and **2b**. These angles are compared favorably with the expected 180° for a terminal carbonyl ligand. These observations imply that the steric interaction between the cation $[\text{M}(\text{Cp})_2\text{H}(\text{CO})]^+$ and the anion $[\text{Co}(\text{CO})_4]^-$ could be neglected.

The mechanism for this reaction may involve initial formation of the dihydrido M(VI) intermediate **A** as a consequence of the heterolytic cleavage of $[\text{Co}_2(\text{CO})_8]$, followed by reductive elimination of $[\text{CoH}(\text{CO})_4]$ to give monohydrido intermediate **B** (Scheme 1). The resulting $[\text{CoH}(\text{CO})_4]$ is known to be highly acidic¹² and may be immediately trapped by $[\text{M}(\text{Cp})_2(\text{H})_2]$, which has been known to be basic and is easily protonated to give cationic trihydride $[\text{M}(\text{Cp})_2(\text{H})_3]^+$, producing intermediate **B**, possibly through the trihydrido intermediate $[\text{M}(\text{Cp})_2(\text{H})_3]^+[\text{Co}(\text{CO})_4]^-$ (**C**) with a subsequent dehydrogenation.⁸ The reaction of **B** with carbon monoxide, which is formed by the decomposition of $[\text{Co}(\text{CO})_4]^-$, may afford the complex **2**. In support of this presumed pathway, we previously reported that the reaction of $[\text{Mo}(\text{Cp})_2(\text{H})_2]$ with TsOH (*p*-toluenesulfonic acid) affords molybdenum trihydride complex $[\text{Mo}(\text{Cp})_2(\text{H})_3]^+(\text{OTs})^-$ and that this complex reacts with carbon monoxide to give $[\text{Mo}(\text{Cp})_2\text{H}(\text{CO})]^+(\text{OTs})^-$,⁸ which has the same cationic moiety as **2a**.

We carried out the reaction of $[\text{W}(\text{Cp})_2(\text{H})_2]$ (**1b**) with $[\text{Co}_2(\text{CO})_8]$ at -40°C in order to observe the possible intermediates. Inspection of the bulk solid recovered from the low temperature reaction mixture by ^1H NMR spectrum showed the existence of two components. One is **2b** and the other is the trihydride $[\text{W}(\text{Cp})_2(\text{H})_3]^+$ species. The hydride resonances of this complex appeared at $\delta = -5.9$ (t, 1H, $J = 8.5$ Hz) and $\delta = -6.6$ (d, 2H), both with ^{183}W satellites ($^1J_{\text{WH}} = 68$ and 46 Hz respectively). Such patterns have been observed previously, and are considered to be characteristic of $[\text{W}(\text{Cp})_2(\text{H})_3]^+$ species.⁸ These results suggest that $[\text{M}(\text{Cp})_2(\text{H})_2]$ are protonated with $[\text{CoH}(\text{CO})_4]$, which is formed by reductive elimination of $[(\text{Cp})_2(\text{H})_2\text{MCo}(\text{CO})_4]^+$ intermediate **A**, to give $[\text{M}(\text{Cp})_2(\text{H})_3]^+[\text{Co}(\text{CO})_4]^-$. Monitoring the reaction of molybdenum complex $[\text{Mo}(\text{Cp})_2(\text{H})_2]$ with

Table 1. Selected Interatomic Distances (Å) and Angles (°) for Complexes **2a** and **2b**

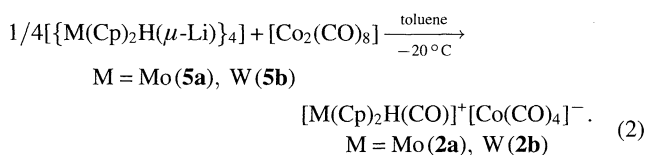
$[\text{Mo}(\text{Cp})_2\text{H}(\text{CO})]^+[\text{Co}(\text{CO})_4]^-$ (2a)		$[\text{W}(\text{Cp})_2\text{H}(\text{CO})]^+[\text{Co}(\text{CO})_4]^-$ (2b)	
Mo1–H1	1.71(9)	W1–H1	1.398(1)
Mo1–CP1	1.917	W1–CP1	1.920
Mo1–CP2	1.957	W1–CP2	1.978
Mo1–C11	1.98(2)	W1–C11	1.98(2)
C11–O11	1.13(1)	C11–O11	1.15(3)
Co1–C21	1.69(2)	Co1–C21	1.73(2)
Co1–C22	1.73(2)	Co1–C22	1.74(3)
Co1–C23	1.70(2)	Co1–C23	1.73(4)
Co1–C24	1.69(2)	Co1–C24	1.74(3)
C21–O21	1.16(2)	C21–O21	1.10(4)
C22–O22	1.17(2)	C22–O22	1.15(4)
C23–O23	1.18(2)	C23–O23	1.11(5)
C24–O24	1.18(2)	C24–O24	1.11(4)
H1–Mo1–C11	81(3)	H1–W1–C11	77(6)
CP1–Mo1–CP2	145.7	CP1–W1–CP2	142.5
Mo1–C11–O11	177(2)	W1–C11–O11	178(2)
Co1–C21–O21	177(2)	Co1–C21–O21	179(3)
Co1–C22–O22	177(2)	Co1–C22–O22	179(5)
Co1–C23–O23	179(2)	Co1–C23–O23	174(4)
Co1–C24–O24	179(2)	Co1–C24–O24	179(2)



Scheme 1.

$[Co_2(CO)_8]$ by low-temperature NMR spectroscopy failed to reveal the presence of any trihydride species, possibly due to the highly labile nature of the $[Mo(Cp)_2(H)_3]^+$ species.

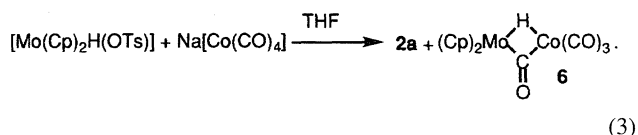
We carried out the syntheses of the complexes **2** by employing other molybdenocene and tungstenocene derivatives as starting materials. Reactions of more active lithium complexes $[M(Cp)_2H(\mu-Li)]_4$ ($M=Mo$ (**5a**), W (**5b**)), which were prepared by treatment of **1a** and **1b** with $n-BuLi$,¹³ with $[Co_2(CO)_8]$ in toluene at $-20^\circ C$ gave **2a** and **2b** in good yields (72 and 69% respectively) (Eq. 2).



Possible reaction pathways are shown in Scheme 2. The initial stage of this reaction is formation of the monohydrido $M(IV)$ intermediate **D**. Presumably, the short-lived intermediate **D** rearranges under the reaction conditions to yield **B**. As supporting evidence for the presence of an equilibrium between **D** and **B**, we previously observed that molybdenum- or tungsten-hydridotosylato complex $[M(Cp)_2H(OTs)]$ is in equilibrium in solution with its ionic species $[M(Cp)_2H]^+(OTs)^-$.¹⁴ In contrast to the reaction between

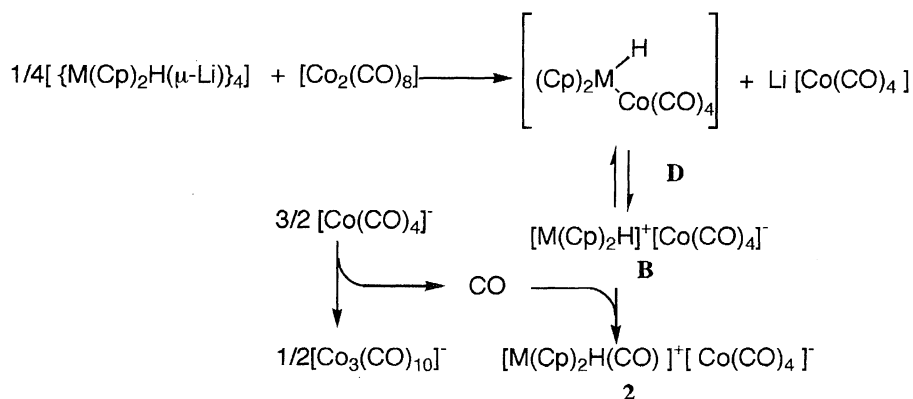
$[M(Cp)_2(H)_2]$ and $[Co_2(CO)_8]$, the formation of trihydride species and $[CoH(CO)_4]$ is not conceivable in this reaction, and the side reactions in which these species are concerned may not take place.

Alternatively, the hydridotosylato complex $[Mo(Cp)_2H(OTs)]$, which is derived from **1a** and an equimolar amount of $TsOH$,⁸ reacted with $Na[Co(CO)_4]$ to give **2a** (41%) and a neutral dinuclear complex $[Mo(Cp)_2(\mu-H)(\mu-CO)Co(CO)_3]$ (**6**) (19%) (Eq. 3). This complex has already been synthesized by the reaction of carbon dioxide complex $[Mo(Cp)_2(\eta^2-CO_2)]$ with $[CoH(CO)_4]$.^{4,5}



Irradiation of $[Mo(Cp)_2(H)_2]$ with $[Co_2(CO)_8]$ in toluene at ambient temperature afforded **2a** (69%) and $[Mo(Cp)_2H(CO)]^+[Co_3(CO)_{10}]^-$ (20%). The IR spectrum of this cluster complex shows three bands at 2030, 1880, and 1600 cm^{-1} , assignable to C–O bands, which are typical for $[Co_3(CO)_{10}]^-$ fragment.¹⁵

Dihydrides $[M(Cp)_2(H)_2]$ are known to react with alkynes to give olefin complexes.¹⁶ In addition, bridged alkyne complexes have been synthesized by the reaction of alkynes



Scheme 2.

with $[\text{Co}_2(\text{CO})_8]$.¹⁷⁾ We therefore tried the reaction of $[\text{W}(\text{Cp})_2(\text{H})_2]$ with $[\text{Co}_2(\text{CO})_8]$ in the presence of diphenylacetylene.

This reaction provided complex **2b** in 73% yield. However we were not able to isolate any alkyne- or olefin-complexes from the reaction mixture.

Finally, some reactivities of the complex **2a** were investigated. The ^1H NMR tube reaction indicated that irradiation of **2a** in THF for 4 h caused no significant change. Although Nicholas reported that the complex **2a** slowly converts to the complex **6** in CH_2Cl_2 /pentane at -20°C , we were not able to observe such transformation.⁴⁾

Experimental

All manipulations were conducted under purified argon or nitrogen. Air-sensitive reagents and products were handled by standard Schlenk techniques. Solvents were dried and purified in the usual manner, and stored under an atmosphere of argon. Commercially available chemicals were used as such without any further purification. UV-visible light irradiation was performed by using a Riko 400-W high-pressure mercury lamp and Pyrex glass filter.

Infrared spectra were determined on a Perkin-Elmer 1600 series spectrometer using KBr disks prepared under inert atmosphere. NMR spectra were recorded on a JEOL JNMEX-270 spectrometer. ^1H NMR chemical shifts were referenced to tetramethylsilane (TMS).

Literature methods were used to prepare $[\text{Mo}(\text{Cp})_2(\text{H})_2]$,¹⁸⁾ $[\text{W}(\text{Cp})_2(\text{H})_2]$,¹⁸⁾ $[\{\text{Mo}(\text{Cp})_2\text{H}(\mu\text{-Li})\}_4]$,¹³⁾ $[\{\text{W}(\text{Cp})_2\text{H}(\mu\text{-Li})\}_4]$,¹³⁾ and $[\text{Mo}(\text{Cp})_2\text{H}(\text{OTs})]$.⁶⁾

X-Ray Crystallographic Studies of 2a,b. Crystals of complexes **2a,b** suitable for diffraction analyses were grown in

THF– Et_2O . The orange crystals thus obtained were mounted in glass capillary tubes under argon. The unit-cell parameters were obtained by least-squares refinement of 2θ values of reflections with $5.0^\circ \leq 2\theta \leq 50.0^\circ$. Intensities were collected on a Rigaku AFC-5R four-circle diffractometer. Mo $K\alpha$ radiations were used ($\lambda = 0.71069 \text{ \AA}$). The parameters used during the collection of diffraction data are given in Table 2.

Calculations were carried out with the program systems teXsan (**2a**) or Crystan (**2b**) on a FACOM A-70 computer. The structures were solved and expanded by using Fourier techniques. The non-hydrogen atoms were refined anisotropically. Hydrogen atoms were included but not refined. Final results are summarized in Tables 3 and 4. The complete data for anisotropic thermal factors in the form Uij are deposited as Document No. 70001 at the Office of the Editor of Bull. Chem. Soc. Jpn.

Preparation of $[\text{Mo}(\text{Cp})_2\text{H}(\text{CO})]^+[\text{Co}(\text{CO})_4]^-$ (2a**) and $[\text{W}(\text{Cp})_2\text{H}(\text{CO})]^+[\text{Co}(\text{CO})_4]^-$ (**2b**).** **Procedure A.** $[\text{Mo}(\text{Cp})_2(\text{H})_2]$ (**1a**) (0.78 g, 3.42 mmol) and $[\text{Co}_2(\text{CO})_8]$ (0.58 g, 1.7 mmol) were placed into a Schlenk flask. THF (50 ml) was added slowly at -78°C and the mixture was stirred at the same temperature. The resultant solution was then heated at room temperature over a period of 4 h. From the reaction mixture, the solvent was evaporated to dryness under reduced pressure. The dark-green precipitate thus obtained was extracted with THF (25 ml) and precipitated by adding Et_2O (25 ml)–hexane (50 ml). The resulting solid was filtered off and dried in vacuo. The other powder thus obtained was $[\text{Mo}(\text{Cp})_2\text{H}(\text{CO})]^+[\text{Co}(\text{CO})_4]^-$ (0.73 g, 50%). This procedure is also applicable to the synthesis of the tungsten analog **2b**, $[\text{W}(\text{Cp})_2\text{H}(\text{CO})]^+[\text{Co}(\text{CO})_4]^-$ (yield=43%).

Procedure B. $[\{\text{W}(\text{Cp})_2\text{H}(\mu\text{-Li})\}_4]$ (**5b**) (0.39 g, 0.3 mmol) suspended in 40 ml of toluene was reacted with $[\text{Co}_2(\text{CO})_8]$ (0.41 g, 1.2 mmol) in 20 ml of toluene at -20°C . After 4 h, the solvent was

Table 2. Experimental Data for the Crystallographic Analysis of Complexes **2a** and **2b**

Compd	2a	2b
Formula	$\text{C}_{15}\text{H}_{11}\text{O}_5\text{CoMo}$	$\text{C}_{15}\text{H}_{11}\text{O}_5\text{CoW}$
MW	426.12	514.03
Crystal system	Monoclinic	Monoclinic
Space group	$P2_1/c$	$P2_1/c$
$a/\text{\AA}$	11.265(12)	11.310(4)
$b/\text{\AA}$	9.055(20)	8.993(3)
$c/\text{\AA}$	15.942(27)	15.896(3)
$\alpha/^\circ$	90.00	90.00
$\beta/^\circ$	93.91(14)	93.21(2)
$\gamma/^\circ$	90.00	90.00
$V/\text{\AA}^3$	1622.4(5)	1614.3(8)
Z	4	4
$F(000)$	840.00	968.00
μ/cm^{-1}	17.925	78.168
$D_{\text{cal}}/\text{g cm}^{-3}$	1.744	2.106
Crystal size/mm	$0.1 \times 0.1 \times 0.1$	$0.3 \times 0.3 \times 0.7$
2θ range/deg	$5.00 < 2\theta < 50.00$	$5.00 < 2\theta < 50.00$
Scan rate/deg min $^{-1}$	8	8
h, k, l Range	$0 < h < 13, 0 < k < 11, -19 < l < 19$	$0 < h < 13, 0 < k < 11, -20 < l < 20$
Unique reflections	2290	3537
Used selections [$F_o > 3\sigma(F_o)$]	849	2655
No. of variables	204	199
R	0.041	0.041
R'	0.040	0.0634
Weighting scheme	0.3614	0.4568

Table 3. Fractional Atomic Coordinates and $B_{\text{iso}}/B_{\text{eq}}$ Values (\AA) for Complex **2a**

Atom	<i>x/a</i>	<i>y/b</i>	<i>z/c</i>	<i>B</i>
Mo1	0.20363(11)	0.19963(14)	0.423519(79)	4.71(8)
Co1	0.28962(20)	−0.33414(25)	0.23453(13)	5.9(1)
O11	0.1150(11)	0.0880(13)	0.24567(72)	9.2(8)
O21	0.2139(15)	−0.6198(16)	0.17783(82)	13(1)
O22	0.3192(12)	−0.1462(15)	0.09037(88)	11(1)
O23	0.5114(13)	−0.3657(20)	0.33293(87)	14(1)
O24	0.1066(14)	−0.2234(15)	0.33490(94)	13(1)
C1	0.0119(21)	0.2656(33)	0.4128(17)	10(2)
C2	0.0411(21)	0.2399(22)	0.4999(21)	10(2)
C3	0.1227(21)	0.3456(25)	0.52284(94)	7(1)
C4	0.1520(17)	0.4330(19)	0.4544(17)	7(1)
C5	0.0735(21)	0.3852(27)	0.3897(13)	7(1)
C6	0.3552(23)	0.0347(41)	0.4667(42)	13(2)
C7	0.3573(22)	0.0659(52)	0.3792(22)	10(2)
C8	0.3834(18)	0.2108(53)	0.3693(17)	9(2)
C9	0.3931(18)	0.2770(32)	0.4423(35)	10(2)
C10	0.3743(24)	0.1716(64)	0.5029(19)	11(2)
C11	0.1438(16)	0.1293(17)	0.31097(97)	7(1)
C21	0.2471(18)	−0.5052(23)	0.2020(11)	8(1)
C22	0.3050(15)	−0.2189(20)	0.1494(12)	8(1)
C23	0.4209(18)	−0.3514(21)	0.2923(11)	8(1)
C24	0.1819(16)	−0.2677(20)	0.2930(11)	8(1)
H11	0.1320(79)	0.044(10)	0.4536(55)	5(3)
H1	−0.0545	0.2116	0.3829	10.6
H2	0.0079	0.1695	0.5403	10.0
H3	0.1619	0.3608	0.5799	8.5
H4	0.2041	0.5208	0.4546	8.2
H5	0.0597	0.4282	0.3350	8.0
H6	0.3456	−0.0689	0.4889	13.5
H7	0.3506	−0.0037	0.3343	11.3
H8	0.4036	0.2689	0.3198	10.0
H9	0.4193	0.3742	0.4644	12.0
H10	0.3790	0.1722	0.5650	12.8

Table 4. Fractional Atomic Coordinates and $B_{\text{iso}}/B_{\text{eq}}$ Values (\AA) for Complex **2b**

Atom	<i>x/a</i>	<i>y/b</i>	<i>z/c</i>	<i>B</i>
W1	0.20233(5)	0.19854(7)	0.42287(3)	4.50(2)
Co1	0.28818(25)	−0.33218(32)	0.23208(16)	5.81(7)
O11	0.11655(22)	0.08445(23)	0.24394(12)	10.21(72)
O21	0.22164(31)	−0.62049(31)	0.17586(14)	12.69(**)
O22	0.31924(21)	−0.14200(39)	0.08847(17)	11.66(87)
O23	0.50161(26)	−0.35122(41)	0.33426(21)	14.03(**)
O24	0.10371(26)	−0.22572(28)	0.33110(21)	11.85(98)
C1	0.00987(24)	0.26340(43)	0.41564(23)	8.51(93)
C2	0.04583(31)	0.24816(33)	0.50398(21)	8.43(85)
C3	0.12844(36)	0.34837(36)	0.52521(14)	8.78(99)
C4	0.14951(21)	0.43706(23)	0.45172(19)	7.47(71)
C5	0.07255(23)	0.38453(26)	0.38685(13)	6.75(62)
C6	0.35827(27)	0.04793(51)	0.46793(26)	10.00(**)
C7	0.35548(21)	0.05699(36)	0.38094(22)	8.46(89)
C8	0.38103(26)	0.21296(48)	0.36607(22)	9.44(**)
C9	0.39301(35)	0.28694(49)	0.44651(32)	10.52(**)
C10	0.37985(32)	0.17552(54)	0.50275(29)	9.85(**)
C11	0.14579(18)	0.12678(22)	0.30998(13)	5.98(52)
C21	0.24699(28)	−0.50747(26)	0.19702(15)	7.61(75)
C22	0.30783(22)	−0.21703(31)	0.14602(19)	7.32(71)
C23	0.41511(34)	−0.34714(38)	0.29730(22)	9.61(**)
C24	0.17510(29)	−0.26886(30)	0.29282(18)	8.26(80)
H11	0.13036(0)	0.07837(0)	0.44227(0)	6.00(**)
H1	−0.04595(0)	0.20178(0)	0.38421(0)	8.49(**)
H2	0.01477(0)	0.17272(0)	0.54088(0)	8.34(**)
H3	0.16561(0)	0.35865(0)	0.58070(0)	8.74(**)
H4	0.20722(0)	0.51729(0)	0.44737(0)	7.49(**)
H5	0.06574(0)	0.42405(0)	0.32966(0)	6.77(**)
H6	0.34537(0)	−0.03740(0)	0.50237(0)	9.99(**)
H7	0.34188(0)	−0.02081(0)	0.34107(0)	8.45(**)
H8	0.38755(0)	0.26312(0)	0.31277(0)	9.41(**)
H9	0.40802(0)	0.39651(0)	0.45468(0)	10.53(**)
H10	0.38347(0)	0.20063(0)	0.56228(0)	9.90(**)

evaporated to dryness under reduced pressure and the residual solid was washed with hexane and ether. The powder thus obtained was $[\text{W}(\text{Cp})_2\text{H}(\text{CO})]^+[\text{Co}(\text{CO})_4]^-$ (**2b**) (0.44 g, 69%). This procedure is also applicable to the synthesis of the molybdenum analog **2a**, $[\text{Mo}(\text{Cp})_2\text{H}(\text{CO})]^+[\text{Co}(\text{CO})_4]^-$ (yield=72%).

Procedure C. A solution containing $[\text{Mo}(\text{Cp})_2\text{H}(\text{OTs})]$ (0.48 g, 1.2 mmol) and $\text{Na}[\text{Co}(\text{CO})_4]$ (0.29 g, 1.5 mmol) in THF (40 ml) was stirred at room temperature. During the stirring, the solution changed from red-brown to orange. After 24 h, the solvent was evaporated to dryness under reduced pressure and the residual solid was washed with hexane and ether, then extracted with THF (30 ml) and reprecipitated by adding Et_2O (15 ml). The precipitate thus obtained was separated by filtration and dried in vacuo. The resultant powder was $[\text{Mo}(\text{Cp})_2\text{H}(\text{CO})]^+[\text{Co}(\text{CO})_4]^-$ (**2a**) (yield=41%). From the mother liquors, the solvent was evaporated to dryness under reduced pressure and the residual solid was washed with hexane. The red-brown powder thus obtained was $[\text{Mo}(\text{Cp})_2(\mu\text{-H})(\mu\text{-CO})\text{Co}(\text{CO})_3]$ (**6**) (19%).

Procedure D. A Pyrex Schlenk flask containing a solution of $[\text{Mo}(\text{Cp})_2(\text{H})_2]$ (**1a**) (0.26 g, 1.2 mmol) and $[\text{Co}_2(\text{CO})_8]$ (0.39 g, 1.2 mmol) dissolved in THF (30 ml) was irradiated by light for 3 h. A continuous stream of argon was passed through the vessel at all times. The solvent was evaporated from the resulting solution to dryness under reduced pressure. The residue was washed with hex-

ane and dried under vacuum. The resulting solid was extracted with THF and reprecipitated by adding Et_2O . The powder thus obtained was $[\text{Mo}(\text{Cp})_2\text{H}(\text{CO})]^+[\text{Co}(\text{CO})_4]^-$ (**2a**) (yield=69%). From the mother liquors, the solvent was evaporated to dryness under reduced pressure and the residual solid was washed successively with Et_2O and acetone, then dried under vacuum. The dark-green powder thus obtained was $[\text{Mo}(\text{Cp})_2\text{H}(\text{CO})]^+[\text{Co}_3(\text{CO})_{10}]^-$ (yield=20%). ^1H NMR (THF- d_8) δ =5.7 (10H, s), −8.2 (1H, s); IR (KBr) 2030, 1880, and 1600 cm^{-1} .

Procedure E. A solution of complex **1b** (0.40 g, 1.3 mmol) in 30 ml of toluene was stirred and cooled to −20 °C. Then a cooled (−20 °C) solution of $[\text{Co}_2(\text{CO})_8]$ (0.27 g, 0.79 mmol) in 20 ml of toluene was added to the solution, followed by the addition of an excess of diphenylacetylene (0.63 g, 3.54 mmol). The solution was stirred for 4 h, while it was warmed to room temperature, and was then filtered. The resulting solid was washed with toluene and was crystallized from THF- Et_2O -hexane. $[\text{W}(\text{Cp})_2\text{H}(\text{CO})]^+[\text{Co}(\text{CO})_4]^-$ was thus isolated in 73% yield.

This work was supported by Grant-in-Aid for Scientific Research on Priority Area No. 05236104 and in part by Grant-in-Aid for Scientific Research (B) No. 07455354 from the Ministry of Education, Science, Sports and Culture.

References

- 1) F. Piacenti, M. Bianchi, and M. Bendetti, *Chim. Ind. (Milan)*, **49**, 245 (1969).
- 2) R. Davis and L. A. P. Kane-Maguire, "Comprehensive Organometallic Chemistry," ed by G. Wilkinson, F. G. A. Stone, and E. W. Abel, Oxford, U.K. (1982), Vol. 3, p. 1198.
- 3) Y. Mugnier and C. Moise, *J. Organomet. Chem.*, **248**, C33 (1983).
- 4) J.-C. Tsai, M. A. Khan, and K. M. Nicholas, *Organometallics*, **10**, 29 (1991).
- 5) J.-C. Tsai, R. A. Weeler, M. A. Khan, and K. M. Nicholas, *Organometallics*, **10**, 1344 (1991).
- 6) M. Minato, H. Tomita, T. Igarashi, J.-G. Ren, T. Tokunaga, and T. Ito, *J. Organomet. Chem.*, **473**, 149 (1994).
- 7) J.-G. Ren, H. Tomita, M. Minato, T. Ito, K. Osakada, and M. Yamasaki, *Organometallics*, **15**, 852 (1996).
- 8) T. Igarashi and T. Ito, *Chem. Lett.*, **1985**, 1699.
- 9) M. A. Adams, K. Folting, J. C. Huffman, and K. G. Caulton, *Inorg. Chem.*, **18**, 3020 (1979).
- 10) J. A. Dean, "Lange's Handbook of Chemistry," McGraw-Hill Book Co., New York (1985).
- 11) D. P. Schussler, W. R. Robinson, and W. F. Edgell, *Inorg. Chem.*, **13**, 153 (1974).
- 12) J. P. Collman, L. S. Hegedus, J. R. Norton, and R. G. Finke, "Principles and Applications of Organotransition Metal Chemistry," University Science Books, Mill Valley, California (1987), p. 91.
- 13) B. R. Francis, M. L. H. Green, T. Luong-thi, and G. A. Moser, *J. Chem. Soc., Dalton Trans.*, **1976**, 1339.
- 14) M. Minato, H. Tomita, J.-G. Ren, and T. Ito, *Chem. Lett.*, **1993**, 1191.
- 15) S. A. Fieldhouse, B. H. Freeland, C. D. M. Mann, and R. J. O'Brien, *J. Chem. Soc., Chem. Commun.*, **1970**, 181.
- 16) A. Nakamura and S. Otsuka, *J. Am. Chem. Soc.*, **94**, 1886 (1972).
- 17) C. Elschenbroich and A. Salzer, "Organometallics. A Concise Introduction," VCH, Weinheim (1989), p. 275.
- 18) M. L. H. Green, J. A. McCleverty, L. Pratt, and G. Wilkinson, *J. Chem. Soc.*, **1961**, 4854.